RESEARCH COMMUNICATION

Two small regulatory RNAs establish opposing fates of a developmental axis

Fabio T.S. Nogueira,[1,3] Shahinez Madi,[1,3] Daniel H. Chitwood,[1,2] Michelle T. Juarez,[1,4] and Marja C.P. Timmermans[1,2,5]

[1]Cold Spring Harbor Laboratory, Cold Spring Harbor, New York 11724, USA; [2]Watson School of Biological Sciences, Cold Spring Harbor, New York 11724, USA

Small RNAs are important regulators of gene expression. In maize, adaxial/abaxial (dorsoventral) leaf polarity is established by an abaxial gradient of microRNA166 (miR166), which spatially restricts the expression domain of class III homeodomain leucine zipper (HD-ZIPIII) transcription factors that specify adaxial/upper fate. Here, we show that *leafbladeless1* encodes a key component in the *trans*-acting small interfering RNA (ta-siRNA) biogenesis pathway that acts on the adaxial side of developing leaves and demarcates the domains of *hd-zipIII* and miR166 accumulation. Our findings indicate that tasiR-ARF, a ta-siRNA, and miR166 establish opposing domains along the adaxial–abaxial axis, thus revealing a novel mechanism of pattern formation.

Supplemental material is available at www.genesdev.org.

Received January 8, 2007; revised version accepted February 20, 2007.

In both animals and plants, many developmentally important regulatory genes are predicted targets of microRNAs (miRNAs), which suggests that such small RNAs constitute a class of developmental determinants (Alvarez-Garcia and Miska 2005; Jones-Rhoades et al. 2006). Patterning and outgrowth of lateral organs in plants depend on the specification of adaxial/abaxial (dorsoventral) polarity in the incipient primordium. This asymmetry is established through the polarized expression of class III homeodomain leucine zipper (HD-ZIPIII) transcription factors that specify adaxial/upper cell fate (McConnell et al. 2001; Emery et al. 2003; Juarez et al. 2004a). The adaxial-specific expression of *hd-zipIII* family members is delineated by the expression pattern of a 21-nucleotide (nt) miRNA, miR166, which directs the cleavage of *hd-zipIII* transcripts (Juarez et al. 2004a; Kidner and Martienssen 2004). In maize, miR166 accumulates most abundantly immediately below the incipient leaf, but a gradient of miR166 extends into the abaxial side of the initiating organ that establishes organ polarity (Juarez et al. 2004a).

[*Keywords*: Meristem; leaf; polarity; pattern formation; microRNA; *trans*-acting siRNA]

[3]**These authors contributed equally to this work.**
[4]**Present address: Cell and Developmental Biology, University of California, San Diego, 9500 Gilman Drive, La Jolla, CA 92093, USA**
[5]**Corresponding author.**
E-MAIL timmerma@cshl.edu; FAX (516) 367-8369.
Article is online at http://www.genesdev.org/cgi/doi/10.1101/gad.1528607.

Specification of adaxial/abaxial organ polarity in maize also requires the activity of *leafbladeless1* (*lbl1*). Recessive mutations in *lbl1* lead to a variable abaxialization of leaves (Timmermans et al. 1998). The weak *lbl1-ref* allele causes a partial loss of adaxial identity revealed as patches of abaxial cells on the upper leaf surface, whereas leaves of the severe *ragged seedling1* allele (*lbl1-rgd1*) are often radially symmetric and completely abaxialized (Fig. 1A). Expression of the *hd-zipIII* family member *rld1* is reduced in *lbl1* mutants. Conversely, increased levels of *hd-zipIII* expression in *Rld1-O* mutants, which carry a miR166-insensitive allele of *rld1*, can fully suppress the vegetative defects of *lbl1* (Juarez et al. 2004b). *lbl1* thus contributes to organ polarity by regulating the accumulation of *rld1* transcripts on the adaxial side of the developing leaf.

Here, we show that *lbl1* encodes a homolog of SUPPRESSOR-OF-GENE-SILENCING3 (SGS3), which is specifically required for the biogenesis of *trans*-acting small interfering RNAs (ta-siRNAs) (Peragine et al. 2004; Vazquez et al. 2004). Ta-siRNAs are derived from noncoding *TAS* transcripts that are initially targeted for cleavage by specific miRNAs (Allen et al. 2005). However, unlike most miRNA-directed cleavage products, *TAS* cleavage fragments are converted into double-stranded RNAs through the activities of SGS3 and RNA-DEPENDENT RNA POLYMERASE6 (RDR6), and subsequently processed by DICER-LIKE4 (DCL4) into 21-base-pair (bp) siRNAs that guide the cleavage of target transcripts, similar to the action of miRNAs (Allen et al. 2005; Gasciolli et al. 2005; Xie et al. 2005; Yoshikawa et al. 2005).

The *Arabidopsis* ta-siRNAs, ta-siR2141, and ta-siR2142 (referred to hereafter as tasiR-ARF), regulate expression of the *AUXIN RESPONSE FACTOR* (*ARF*) genes *ARF3* and *ARF4* (Allen et al. 2005; Williams et al. 2005). These transcription factors act redundantly to promote abaxial fate, inferring a role for the ta-siRNA pathway in leaf polarity (Pekker et al. 2005). However, a role for ta-siRNAs in leaf polarity remains tentative, as *Arabidopsis* mutants that block ta-siRNA biogenesis, such as *sgs3*, develop no obvious leaf polarity defects (Peragine et al. 2004; Adenot et al. 2006; Hunter et al. 2006). Here, we demonstrate an essential role for the maize ta-siRNA pathway in the specification of adaxial fate. We show that tasiR-ARF accumulates on the adaxial side of developing leaf primordia and restricts the expression domain of abaxial determinants, including miR166. As miR166 defines the abaxial side of the leaf, our results reveal a novel mechanism of pattern formation in which asymmetry along a developmental axis is determined by two opposing small RNAs.

Results and Discussion

Members of the *hd-zipIII* family contribute redundantly to adaxial fate (Emery et al. 2003; Juarez et al. 2004b). To assess whether loss of adaxial identity in *lbl1* is associated with altered expression of *hd-zipIII* family members other than *rld1*, we compared the expression pattern of *rolled leaf2* (*rld2*) in wild-type and *lbl1-rgd1* mutant apices. *rld2* is normally expressed at the tip of the shoot apical meristem (SAM), in the vasculature, and along the adaxial side of developing leaf primordia (Fig. 1B). This

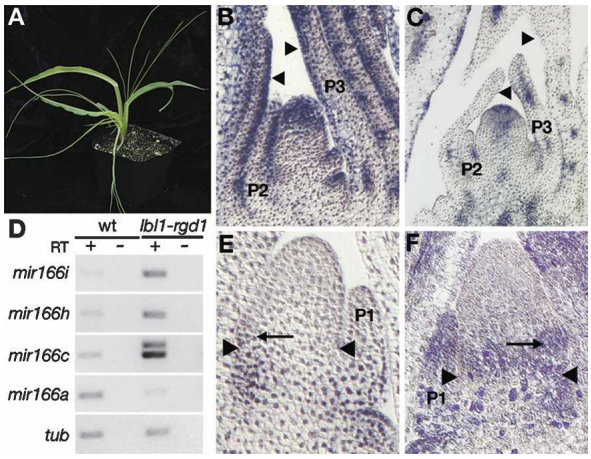

Figure 1. *leafbladeless1* (*lbl1*) establishes leaf polarity by demarcating the domains of *hd-zipIII* and miR166 expression. (*A*) *lbl1-rgd1* seedling with thread-like abaxialized leaves. (*B*) Longitudinal section through a wild-type apex shows *rld2* expression in the SAM, vasculature, and adaxially in leaf primordia (arrowheads). (*C*) In *lbl1-rgd1*, meristematic, and adaxial (arrowheads) *rld2* expression is reduced. (*D*) Precursor levels for *mir166i*, *mir166h*, and *mir166c* are increased in *lbl1-rgd1* compared with wild type, whereas expression of *mir166a* is reduced. (*E*) In wild type, miR166 is expressed below and on the abaxial side of the incipient leaf (arrow). (*F*) In *lbl1-rgd1*, miR166 is expressed at the base of the SAM and uniformly throughout the incipient (arrow) and P1 primordia. Arrowheads in *E* and *F* mark the base of the incipient leaf.

expression pattern resembles that of *rld1* and supports a redundant role for these *hd-zipIII* genes in promoting adaxial fate. *rld2* expression in the vasculature is mostly unaffected in *lbl1-rgd1*, but the levels of *rld2* transcripts in the SAM and on the adaxial leaf surfaces are dramatically reduced or lost in *lbl1-rgd1* (Fig. 1C). These observations indicate that *lbl1* contributes to leaf polarity by regulating the adaxial expression of multiple *hd-zipIII* genes. Perhaps *lbl1* regulates *hd-zipIII* expression at the transcriptional level; alternatively, because the *hd-zipIII* expression domain in the leaf is defined by miR166 (Juarez et al. 2004a; Timmermans et al. 2004), *lbl1* could affect *hd-zipIII* expression through changes in the pattern of miR166 accumulation. To test this possibility, we analyzed expression of miR166 in *lbl1-rgd1*.

The maize genome includes at least nine loci, *mir166a* to *mir166i*, with the potential to generate identical copies of the mature miR166. We used RT–PCR to examine the effect of *lbl1* on *mir166* precursor levels in vegetative apices comprising the SAM and four-leaf primordia. Expression levels for *mir166c*, *mir166h*, and *mir166i* are increased in *lbl1-rgd1* as compared with wild type, whereas transcript levels for *mir166a* are reduced in *lbl1-rgd1* (Fig. 1D). Expression levels of the remaining *mir166* family members are unaltered in *lbl1-rgd1*, indicating that *lbl1* affects the accumulation of a specific subset of *mir166* precursors.

We subsequently used in situ hybridization to determine whether the changes in *mir166* transcript levels associated with reduced LBL1 activity also affect the pattern of miR166 accumulation. No hybridization signal was detected using a *mir166a* precursor-specific probe that excludes the mature miRNA (Supplementary Fig. 1). However, consistent with previous results (Juarez et al. 2004a), in situ hybridization with a probe complementary to the mature miR166 showed that the highest concentration of miR166 occurs immediately below the incipient leaf and that miR166 accumulates in a graded pattern on the abaxial side of the initiating organ (Fig. 1E). Expression of miR166 in the region below the incipient leaf is unaffected in *lbl1-rgd1*, but miR166 expression at the site of leaf initiation is markedly changed in this mutant (Fig. 1F). In *lbl1-rgd1*, miR166 is ectopically expressed in a ring at the base of the SAM that overlaps broadly with the incipient leaf. Expression of miR166 in the P1 primordium also persists in a broader domain and includes both the abaxial and adaxial sides. These findings are consistent with the decrease in *hd-zipIII* expression in *lbl1* leaf primordia and indicate a role for *lbl1* in promoting adaxial and/or restricting abaxial fate. They also support a distinct contribution of *lbl1* to *hd-zipIII* expression in the tip of the SAM (Juarez et al. 2004b).

To gain insight into the mechanism with which *lbl1* contributes to leaf polarity, we used a directed transposon-tagging strategy to clone *lbl1*. One novel allele, *lbl1-54*, was recovered that conditions a weak mutant phenotype. Genetic analysis identified a single *Mu8* transposable element that cosegregates with the *lbl1-54* mutation (<0.2 cM) and is absent in the progenitor lines. This *Mu8* element had inserted into the first intron of a gene encoding a protein with high homology with SGS3 (Fig. 2A,B; Mourrain et al. 2000). The maize and *Arabidopsis* proteins share 65% amino acid similarity overall, but the degree of sequence similarity is higher in the Zn-finger (92%) and XS domains (79%) that define the SGS3 family of proteins (Fig. 2B). Consistent with its mild phenotypic effects, the *lbl1-54* insertion allele has a moderate effect on normal transcript levels (Fig. 2C). Sequence analysis of additional mutant alleles confirmed that *lbl1* encodes a SGS3 homolog (Fig. 2A). We found that a single base-pair change in a second intron splice site that reduces the level of normally spliced transcripts distinguishes the weak *lbl1-ref* allele from its progenitor (Fig. 2A,C). *lbl1-rgd1* as well as the severe *lbl1-372* allele result from point mutations that affect *lbl1* expression and cause amino acid substitutions at critical residues of the Zn-finger (Fig. 2A–C; Supplementary Fig. 2).

SGS3 is required for the biogenesis of ta-siRNAs upon miRNA-directed cleavage of *TAS* precursors (Peragine et al. 2004; Vazquez et al. 2004; Allen et al. 2005). Three gene families that generate ta-siRNAs are known in *Arabidopsis*. *TAS1* and *TAS2* precursors are targets of miR173, whereas production of ta-siRNAs from *TAS3* depends on cleavage by miR390 (Allen et al. 2005). Database analysis identified no maize homologs of *TAS1*, *TAS2*, and *MIR173*, but the maize genome includes one *mir390* locus and four *TAS3* homologs, *tas3a–tas3d*, whose transcripts are predicted targets for miR390 (Fig. 3A). RT–PCR analysis showed that all four *tas3* genes as well as *mir390* are expressed in vegetative apices (Fig. 3B). Only subtle differences in the levels of *tas3* transcripts were observed in *lbl1-rgd1* as compared with wild type, but primary transcripts from *mir390* are clearly elevated in *lbl1-rgd1* (Fig. 3B). Because *mir390* is in turn required for ta-siRNA biogenesis, this suggests that negative feedback regulation may exist in the ta-siRNA pathway of maize. Perhaps *mir390* expression is under control of a ta-siRNA target gene.

Ta-siRNAs are generated with a 21-nt phasing starting at the miRNA cleavage site (Fig. 3A; Allen et al. 2005).

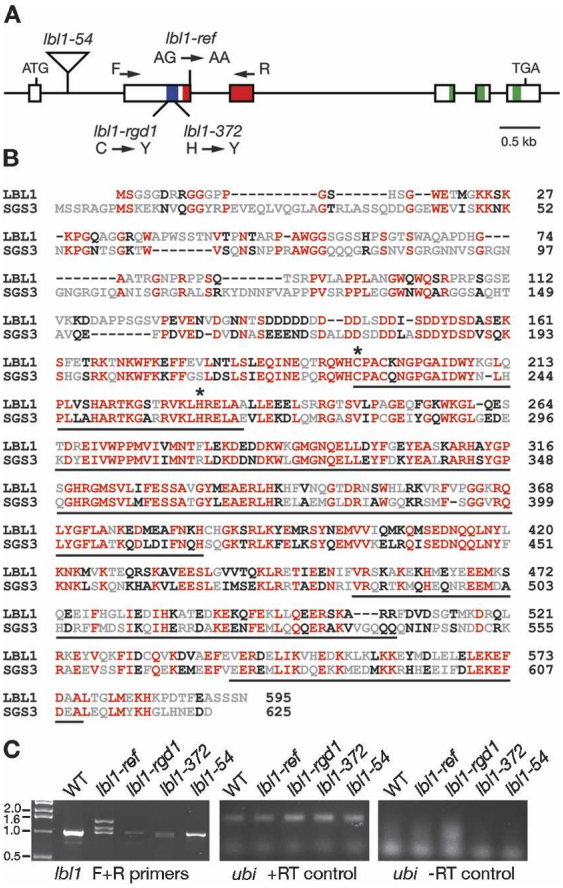

Figure 2. *lbl1* encodes a homolog of SUPPRESSOR-OF-GENE-SILENCING3 (SGS3). (*A*) Diagrammatic representation of the *lbl1* gene. Boxes represent exons, and the zinc-finger, XS, and coil-coiled domains are highlighted in blue, red, and green, respectively. F and R represent primers used for RT–PCR analysis in *C*. Mutations in four mutant *lbl1* alleles are indicated. (C) Cysteine; (H) histidine; (Y) tyrosine. (*B*) Alignment of the maize LBL1 and *Arabidopsis* SGS3 proteins, with red indicating identity and black indicating similarity. The zinc-finger, XS, and coil-coiled domains are underlined, and asterisks mark the amino acids mutated in *lbl1-rgd1* and *lbl1-372*. (*C*) *lbl1* transcript levels are reduced in the mutants compared with wild type. Loading and –RT controls are shown.

Consequently, their sequences as well as potential targets can be predicted using computational approaches. Despite extensive sequence divergence between the *Arabidopsis* and maize *TAS3* genes, the potential for *tas3* transcripts to yield copies of tasiR-ARF is conserved in maize. *tas3a–tas3c* contain two tandemly arranged copies of tasiR-ARF, whereas *tas3d* contains a single tasiR-ARF sequence (Fig. 3A). To establish that LBL1 functions in the biogenesis of ta-siRNAs, we analyzed the accumulation of tasiR-ARF in both wild-type and *lbl1-rgd1* apices (Fig. 3C). Because ta-siRNAs accumulate to unusually low levels in comparison to most miRNAs (Allen et al. 2005; Lu et al. 2006), small RNA blots were hybridized with a 16-nt LNA-modified DNA probe that recognizes tasiR-ARF derived from each of the *tas3* loci (Fig. 3A). tasiR-ARF accumulates to detectable levels only in wild-type apices, suggestive of functional conservation between LBL1 and SGS3 (Fig. 3C).

To substantiate a role for *lbl1* in ta-siRNA biogenesis, we also tested whether loss of LBL1 activity affects the cleavage of ta-siRNA target transcripts. Prospective targets were identified for tasiR-ARF only, and as in *Arabidopsis,* these include four members of the maize *arf3* gene family, referred to herein as *arf3a–arf3d*. We used 5′ RACE to validate *arf3a* as a tasiR-ARF target and to determine the effect of mutations in *lbl1* on ta-siRNA-directed *arf3a* cleavage. *arf3a* contains two tasiR-ARF complementary sites (A and B). RNA from wild-type apices yielded one predominant 5′ RACE product for *arf3a*, resulting from cleavage at positions 9 or 10 of the tasiR-ARF complementary site B (Fig. 3D,E). Importantly, the abundance of this 5′ RACE product is strongly reduced in *lbl1-rgd1* (Fig. 3D), whereas *arf3a* transcript levels are increased in *lbl1-rgd1* apices compared with wild type (Fig. 3B). These data indicate that *arf3a* is a direct target of tasiR-ARF and reveal extensive conservation in the ta-siRNA pathway between maize and *Arabidopsis*.

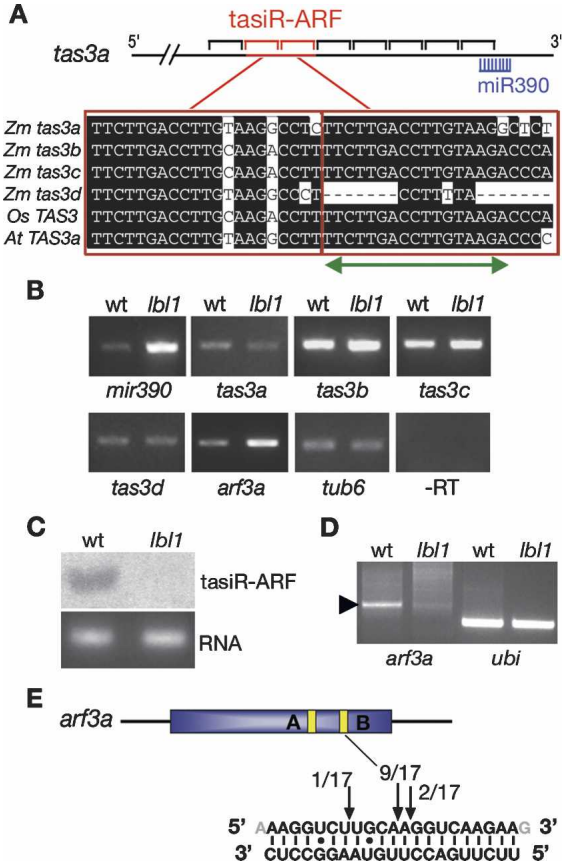

Figure 3. *lbl1* encodes an essential component of the ta-siRNA pathway. (*A*) Diagram of the *tas3a* transcript. The 21-nt intervals phased relative to the miR390 cleavage site are shown as black brackets and the red brackets indicate the positions of tasiR-ARF. An alignment of tasiR-ARF sequences from maize, rice, and *Arabidopsis* is shown *below*, and the green arrow indicates complementarity to the tasiR-ARF LNA probe. Note that *tas3d* also has complementarity to this probe. (*B*) RT–PCR showing the relative expression levels of *mir390*, the *tas3* genes, and *arf3a* in wild-type and *lbl1-rgd1* apices. Loading and –RT controls are shown. (*C*) Small RNA Northern showing that tasiR-ARF accumulates in wild-type, not in *lbl1-rgd1* apices. (*D*) 5′ RACE analysis shows a single prominent *arf3a* cleavage product (arrowhead) only in wild type. RT–PCR of *ubiquitin* served as loading control. (*E*) Diagram of the *arf3a* transcript with tasiR-ARF complementary sites A and B. The 5′ ends of the tasiR-ARF cleavage products map to complementary site B.

Moreover, these data indicate that *lbl1* forms an essential component of the ta-siRNA pathway and implicate this pathway in leaf polarity in maize.

Next, we analyzed the *lbl1* expression pattern by in situ hybridization to determine where in the vegetative apex ta-siRNA biogenesis may occur. *lbl1* expression is most pronounced in a dome of cells at the tip of the meristem that extends into the adaxial side of the initiating primordium (Fig. 4A). In the P1 and P2 primordia, *lbl1* is expressed preferentially on the adaxial side, and during later stages of leaf development, expression of *lbl1* becomes restricted to the margins and vasculature. This expression pattern suggests that ta-siRNAs may accumulate in a defined and perhaps polarized pattern in young leaves. We therefore analyzed the expression pattern of tasiR-ARF using in situ hybridization. In normal apices, hybridization to the tasiR-ARF complementary LNA probe (Fig. 3A) was most pronounced on the adaxial side of incipient and developing leaf primordia (Fig. 4B–D). However, some signal was detectable in *lbl1-rgd1* primordia (Fig. 4E). Because *tas3* precursors, unlike miRNA precursors, are quite abundant, this suggests that the expression pattern in wild-type apices may reflect the accumulation of *tas3* transcripts, in addition to the mature tasiR-ARF. The persistence of *tas3* transcripts in *lbl1-rgd1* (Figs. 3B, 4E) suggests that their expression is regulated independently of the ta-siRNA pathway. More importantly, the expression pattern in wild-type apices suggests that tasiR-ARF and perhaps *tas3* act foremost on the adaxial side of the developing primordia.

Considering the mechanism of ta-siRNA action, such polar expression suggests that the ta-siRNA pathway contributes to leaf polarity in part by restricting the accumulation of abaxial determinants, such as miR166, in a domain of the incipient primordium where adaxial–abaxial polarity is established. To test this possibility, we analyzed the effect of loss of *lbl1* activity on expression of *arf3a* and the *mir166* genes in the SAM. The low abundance of miRNA precursors precludes expression analyses of individual *mir166* genes by in situ hybridization (Supplementary Fig. 1; Juarez et al. 2004a; Kidner and Timmermans 2006). We therefore developed laser capture microdissection (LCM) in combination with RT–PCR to analyze expression of these genes in the apex of wild-type and *lbl1* mutants with high sensitivity and tissue-specific resolution. Cells were captured from the SAM plus the adaxial side of the incipient leaf and, to assess the role of the ta-siRNA pathway during primordium development, from the P1 plus P2 leaves (Fig. 4F). *arf3a* transcripts are undetectable in the wild-type SAM, but *arf3a* is expressed in the SAM of *lbl1-rgd1*. Transcript levels of *arf3a* are also increased in young leaf primordia of *lbl1-rgd1* compared with wild type. This confirms that *lbl1* and the ta-siRNA pathway function to restrict the expression domain of *arf3a* in the SAM, as well as during primordium development. Of the *mir166* genes that are differentially expressed between wild-type and *lbl1* apices (Fig. 1D), primary transcripts for *mir166c* accumulate specifically in the SAM and young leaf primordia of *lbl1-rgd1*, and expression levels for *mir166i* are increased in these mutant tissues (Fig. 4F). This indicates that the ectopic expression of miR166 in *lbl1-rgd1* incipient primordia results from the broadened expression of *mir166c* and/or *mir166i*. Moreover, these data support the notion that the ta-siRNA pathway specifies adaxial fate by spatially defining the expression domains of these *mir166* genes, although perhaps indirectly via regulation of ARF3 transcription factors or other abaxial determinants.

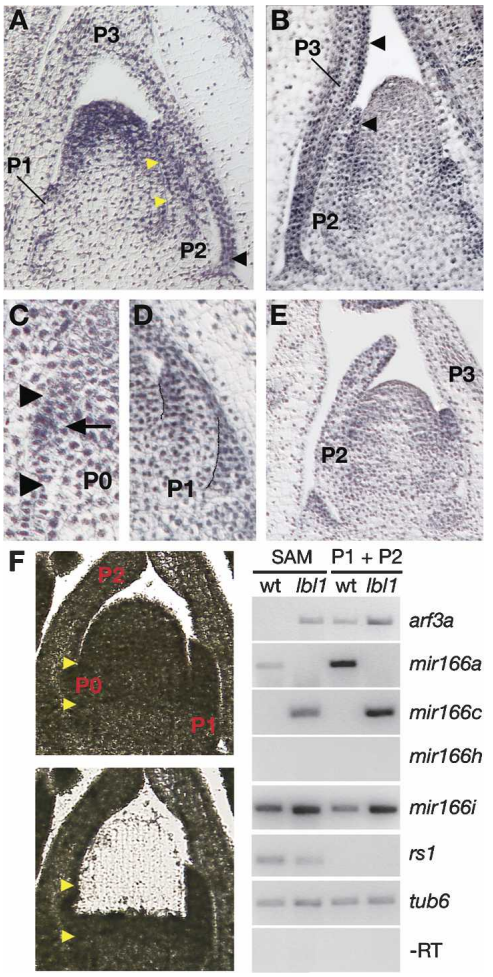

Figure 4. The ta-siRNA pathway acts on the adaxial side of developing leaf primordia and restricts expression of abaxial determinants. (*A*) Longitudinal section through a wild-type apex showing *lbl1* expression in the meristem tip and adaxially in leaf primordia. The yellow arrowheads mark the position of the incipient or P0 primordium, and the black arrowhead indicates expression at the P3 margin. (*B–E*) In situ hybridization with the tasiR-ARF complementary LNA-modified DNA probe in longitudinal sections through wild-type (*B–D*) and *lbl1-rgd1* (*E*) apices. (*B*) In wild type, tasiR-ARF accumulates predominantly on the adaxial side of developing leaves. Arrowheads highlight adaxial expression in P2 and P3 primordia. (*C*) A close-up of a distinct incipient leaf shows adaxial tasiR-ARF expression (arrow). (*D*) A close-up of a P1 primordium also shows adaxial accumulation of tasiR-ARF. (*E*) Some hybridization to the tasiR-ARF complementary LNA probe is observed in *lbl1-rgd1*, perhaps reflecting hybridization to *tas3* precursor transcripts. (*F*, *left* panels) *lbl1-rgd1* apices before and after laser capture microdissection. The incipient leaf is marked by yellow arrowheads. (*Right* panel) RT–PCR analysis on LCM samples of the SAM or P1 plus P2 leaf primordia showing the effect of *lbl1-rgd1* on expression of *arf3a, mir166a*, *mir166c*, and *mir166i*. The SAM-specific homeobox gene *rough sheath1* (*rs1*) was analyzed as LCM control (Schneeberger et al. 1995). Loading and –RT controls are also shown.

Recent studies have shown that tasiR-ARF-mediated cleavage of *ARF3* is required for normal leaf development in *Arabidopsis*, and accordingly, infer a role for the

ta-siRNA pathway in leaf polarity (Fahlgren et al. 2006; Garcia et al. 2006). However, the contribution of this pathway to adaxial–abaxial patterning in *Arabidopsis* remains unclear. In fact, *ARF3* is expressed uniformly throughout young leaf primordia (Pekker et al. 2005), and *Arabidopsis* mutants that block the biogenesis of ta-siRNAs develop no obvious leaf polarity defects (Peragine et al. 2004; Adenot et al. 2006). Moreover, the distribution of trichomes in such mutants as well as in plants expressing a tasiR-ARF-insensitive allele of *ARF3* is inconsistent with the predicted abaxializing phenotype (Fahlgren et al. 2006; Hunter et al. 2006).

Our findings uncover two small RNAs, miR390 and tasiR-ARF, that act upstream of previously known components in the leaf polarity pathway. tasiR-ARF accumulates on the adaxial site of leaf primordia and contributes to organ polarity by spatially restricting the expression domain of abaxial determinants, including miR166, in the incipient and young leaves. This presents the intriguing possibility that distinct small regulatory RNAs direct the establishment of opposing domains along the adaxial–abaxial axis; whereas tasiR-ARF defines the adaxial domain, miR166 delineates the abaxial domain by restricting expression of the adaxializing *HD-ZIPIII* genes. These findings thus reveal a novel patterning mechanism in development.

A function for tasiR-ARF and miR166 in the incipient leaf also raise the question of whether small RNAs contribute to the production or perception of positional information from the SAM required for adaxial–abaxial patterning (Sussex 1951; Reinhardt et al. 2005). tasiR-ARF and miR166 are expressed in essentially complementary domains in the incipient as well as young leaf primordia, consistent with the proposed model that the ta-siRNA pathway, perhaps via *arf3* or other abaxial determinants, spatially restricts the accumulation of miR166 in these tissues (Supplementary Fig. 3). Based on the graded pattern of miR166 accumulation in developing leaf primordia, we previously suggested that a mobile signal controls expression of *mir166* precursors or that miR166 itself acts as a local mobile signal (Juarez et al. 2004a). The loss of this graded polar pattern of expression in *lbl1* mutants and the involvement of the ta-siRNA pathway in the spatial regulation of abaxial determinants is therefore particularly intriguing. The non-cell-autonomous nature of gene silencing is mediated by a distinct branch of the RNA interference (RNAi) machinery (Dunoyer et al. 2005). Ta-siRNA biogenesis utilizes components of this unique RNAi pathway, presenting the possibility that the ta-siRNA pathway may similarly include a non-cell-autonomous component. The unique properties of ta-siRNA biogenesis might also exist to limit tasiR-ARF production, as mature tasiR-ARFs scarcely accumulate despite an abundance of precursor transcripts (Allen et al. 2005; Lu et al. 2006). Their low dose would implicitly affect their efficacy (Bartel 2004; Jones-Rhoades et al. 2006) and, if tasiR-ARFs are themselves able to move, their range of activity (Voinnet 2005). Both may be important variables if a balance between adaxial and abaxial fates is to be struck.

Materials and methods

Cloning of lbl1

lbl1 was cloned using a directed transposon-tagging approach. Please see Supplemental Material for details. Full-length *lbl1* cDNA clones were obtained by RT– and RACE–PCR using total RNA from apices of 2-wk-old seedlings. Mutant *lbl1* alleles were sequenced from RT–PCR products amplified using gene-specific primers that spanned the full-length *lbl1* cDNA.

Sequence analysis

Sequences corresponding to the maize *tas3* and *mir390* loci were assembled using EST and genomic (http://magi.plantgenomics.iastate.edu) databases. Potential ta-siRNA targets were identified in the maize EST data set following the criteria established in Allen et al. (2005). Gene predictions were verified by RT–PCR, RACE, and sequence analysis. The GenBank accession number for *lbl1* is DQ832257, and the MAGIv4 accession numbers are *mir390*, 106773; *tas3a*, 69518; *tas3b*, 65670; *tas3c*, 63185; *tas3d*, PUIFI48.F; and *arf3a*, 48978.

Molecular biology

RNA from vegetative apices including the SAM and four leaf primordia was isolated and analyzed by RT–PCR as described (Juarez et al. 2004b). 5′ RACE was performed as described (Allen et al. 2005). Primer sequences and detailed PCR conditions for all genes analyzed are available upon request. Low-molecular-weight RNA (5 µg) from vegetative apices was extracted, blotted, and hybridized with an end-labeled 16-nt LNA-modified oligonucleotide probe (Exiqon) complementary to tasiR-ARF (CTTA CAAGGTCAAGAA) as described (Allen et al. 2005).

In situ hybridization

In situ hybridizations were performed as described (Kidner and Timmermans 2006). The tasiR-ARF LNA probe was hybridized at 37°C. The *rld2* and *lbl1*probes comprises nucleotides 625–1677 and 120–810 of the coding sequence, respectively, and were used at a concentration of 0.5 ng μL^{-1} kb^{-1}. miR166 probes are as described (Juarez et al. 2004a).

LCM and expression analysis

Shoot apices of 2-wk-old seedlings were embedded as described (http://maize-meristems.plantgenomics.iastate.edu/resources/protocols). Six independent apices were captured for wild-type and *lbl1* samples. LCM was performed using a PALM MicroBeam system. RNA samples were isolated using the PicoPure RNA isolation kit (Arcturus) and amplified using the RiboAmpHS RNA Amplification kit (Arcturus), according to the manufacturer's instructions. RT–PCR was performed on 50–150 ng of amplified, DNase-treated aRNA using the OneStep RT–PCR kit (Qiagen). Primer sequences and PCR conditions are available upon request.

Acknowledgments

We thank Julie Thomas, Krista Marran, and Amanda Grieco for excellent technical assistance; Tim Mulligan for plant care; and Cris Kuhlemeier, Greg Hannon, and members of the Timmermans laboratory for critical reading of the manuscript. This work was supported by grants to M.T. from the USDA (03420) and the NSF (0315676). F.N. was funded in part by a CSHL Association fellowship, S.M. and the LCM experiments were funded by NSF VCA-PGR 0321595, and D.C. is an NSF graduate research fellow and a G. and M. Matheson fellow.

References

Adenot, X., Elmayan, T., Lauressergues, D., Boutet, S., Bouche, N., Gasciolli, V., and Vaucheret, H. 2006. DRB4-dependent *TAS3 trans*-acting siRNAs control leaf morphology through AGO7. *Curr. Biol.* **16:** 927–932.

Allen, E., Xie, Z., Gustafson, A., and Carrington, J. 2005. microRNA-directed phasing during *trans*-acting siRNA biogenesis in plants. *Cell* **121:** 207–221.

Alvarez-Garcia, I. and Miska, E. 2005. MicroRNA functions in animal development and human disease. *Development* **132:** 4653–4662.

Bartel, D. 2004. MicroRNAs: Genomics, biogenesis, mechanism, and function. *Cell* **116:** 281–297.

Dunoyer, P., Himber, C., and Voinnet, O. 2005. DICER-LIKE 4 is required for RNA interference and produces the 21-nucleotide small interfering RNA component of the plant cell-to-cell silencing signal. *Nat. Genet.* **37:** 1356–1360.

Emery, J.F., Floyd, S.K., Alvarez, J., Eshed, Y., Hawker, N., Izhaki, A.,

Baum, S.F., and Bowman, J.L. 2003. Radial patterning of *Arabidopsis* shoots by class III *HD-ZIP* and *KANADI* genes. *Curr. Biol.* **13:** 1768–1774.

Fahlgren, N., Montgomery, T., Howell, M., Allen, E., Dvorak, S., Alexander, A., and Carrington, J. 2006. Regulation of *AUXIN RESPONSE FACTOR3* by *TAS3* ta-siRNA affects developmental timing and patterning in *Arabidopsis*. *Curr. Biol.* **16:** 939–944.

Garcia, D., Collier, S., Byrne, M., and Martienssen, R. 2006. Specification of leaf polarity in *Arabidopsis* via the *trans*-acting siRNA pathway. *Curr. Biol.* **16:** 933–938.

Gasciolli, V., Mallory, A., Bartel, D., and Vaucheret, H. 2005. Partially redundant functions of *Arabidopsis* DICER-like enzymes and a role for DCL4 in producing *trans*-acting siRNAs. *Curr. Biol.* **15:** 1494–1500.

Hunter, C., Willmann, M., Wu, G., Yoshikawa, M., de la Luz Gutierrez-Nava, M., and Poethig, S. 2006. Trans-acting siRNA-mediated repression of *ETTIN* and *ARF4* regulates heteroblasty in *Arabidopsis*. *Development* **133:** 2973–2981.

Jones-Rhoades, M., Bartel, D., and Bartel, B. 2006. MicroRNAs and their regulatory roles in plants. *Annu. Rev. Plant Biol.* **57:** 19–53.

Juarez, M., Kui, J., Thomas, J., Heller, B., and Timmermans, M. 2004a. microRNA-mediated repression of *rolled leaf1* specifies maize leaf polarity. *Nature* **428:** 84–88.

Juarez, M., Twigg, R., and Timmermans, M. 2004b. Specification of adaxial cell fate during maize leaf development. *Development* **131:** 4533–4544.

Kidner, C. and Martienssen, R. 2004. Spatially restricted microRNA directs leaf polarity through ARGONAUTE1. *Nature* **428:** 81–84.

Kidner, C. and Timmermans, M. 2006. In situ hybridization as a tool to study the role of microRNAs in plant development. *Methods Mol. Biol.* **342:** 159–179.

Lu, C., Kulkarni, K., Souret, F., Muthu, V., Tej, S., Poethig, R., Henderson, I., Jacobsen, S., Wang, W., Green, P., et al. 2006. MicroRNAs and other small RNAs enriched in the *Arabidopsis* RNA-dependent RNA polymerase-2 mutant. *Genome Res.* **16:** 1276–1288.

McConnell, J., Emery, J., Eshed, Y., Bao, N., Bowman, J., and Barton, M. 2001. Role of *PHABULOSA* and *PHAVOLUTA* in determining radial patterning in shoots. *Nature* **411:** 709–713.

Mourrain, P., Beclin, C., Elmayan, T., Feuerbach, F., Godon, C., Morel, J., Jouette, D., Lacombe, A., Nikic, S., Picault, N., et al. 2000. *Arabidopsis SGS2* and *SGS3* genes are required for posttranscriptional gene silencing and natural virus resistance. *Cell* **101:** 533–542.

Pekker, I., Alvarez, J., and Eshed, Y. 2005. Auxin response factors mediate *Arabidopsis* organ asymmetry via modulation of KANADI activity. *Plant Cell* **17:** 2899–2910.

Peragine, A., Yoshikawa, M., Wu, G., Albrecht, H., and Poethig, S. 2004. *SGS3* and *SGS2/SDE1/RDR6* are required for juvenile development and the production of *trans*-acting siRNAs in *Arabidopsis*. *Genes & Dev.* **18:** 2368–2379.

Reinhardt, D., Frenz, M., Mandel, T., and Kuhlemeier, C. 2005. Microsurgical and laser ablation analysis of leaf positioning and dorsoventral patterning in tomato. *Development* **132:** 15–26.

Schneeberger, R., Becraft, P., Hake, S., and Freeling, M. 1995. Ectopic expression of the *knox* homeobox gene *rough sheath1* alters cell fate in the maize leaf. *Genes & Dev.* **9:** 2292–2304.

Sussex, I. 1951. Experiments on the cause of dorsiventrality in leaves. *Nature* **167:** 651–652.

Timmermans, M., Schultes, N., Jankovsky, J., and Nelson, T. 1998. *Leafbladeless1* is required for dorsoventrality of lateral organs in maize. *Development* **125:** 2813–2823.

Timmermans, M., Juarez, M., and Phelps-Durr, T. 2004. A conserved microRNA signal specifies leaf polarity. *Cold Spring Harb. Symp. Quant. Biol.* **69:** 409–417.

Vazquez, F., Vaucheret, H., Rajagopalan, R., Lepers, C., Gasciolli, V., Mallory, A., Hilbert, J., Bartel, D., and Crete, P. 2004. Endogenous *trans*-acting siRNAs regulate the accumulation of *Arabidopsis* mRNAs. *Mol. Cell* **16:** 69–79.

Voinnet, O. 2005. Non-cell autonomous RNA silencing. *FEBS Lett.* **579:** 5858–5871.

Williams, L., Carles, C., Osmont, K., and Fletcher, J. 2005. A database analysis method identifies an endogenous *trans*-acting short-interfering RNA that targets the *Arabidopsis ARF2, ARF3*, and *ARF4* genes. *Proc. Natl. Acad. Sci.* **102:** 9703–9708.

Xie, Z., Allen, E., Wilken, A., and Carrington, J. 2005. DICER-LIKE 4 functions in *trans*-acting small interfering RNA biogenesis and vegetative phase change in *Arabidopsis* thaliana. *Proc. Natl. Acad. Sci.* **102:** 12984–12989.

Yoshikawa, M., Peragine, A., Park, M., and Poethig, S. 2005. A pathway for the biogenesis of *trans*-acting siRNAs in *Arabidopsis*. *Genes & Dev.* **19:** 2164–2175.